Int J Pharm Bio Sci 2013 Oct; 4(4): (P) 661 - 674

Research Article **Nanotechnology**

International Journal of Pharma and Bio Sciences **ISSN 0975-6299**

GREEN SYNTHESIS OF SILVER NANOPARTICLES USING LEAVES EXTRACT OF *CENTELLA ASIATICA* L. FOR STUDIES AGAINST HUMAN PATHOGENS

ANANDINI ROUT[1], PADAN KUMAR JENA[1], UMESH KUMAR PARIDA[2] AND BIRENDRA KUMAR BINDHANI*[2]

[1]Department of Botany, Ravenshaw University, Cuttack, Odisha, India
**[2]School of Biotechnology, KIIT University, Bhubaneswar, Odisha, India*

ABSTRACT

There is an ever-increasing commercial demand for nanoparticles due to their extensive applicability in various markets, including medicine, catalysis, electronics, chemistry, and energy. In this report, a simple and eco-friendly chemical reaction for the green synthesis of silver nanoparticles from *Centella asiatica* L. has been developed. Here we report for the first time, to the best of our knowledge, the synthesis of silver nanoparticles of varying sizes using aqueous extract of leaves of *Centella asiatica* L. at room temperature. The synthesized nanoparticles are evaluated for its antimicrobial activity against human pathogens, *Staphylococcus aureus* (MTCC 9542) which is a common agent for skin infections. Synthesized nanoparticles were characterized using UV-visible spectrophotometer, Fourier Transmission Infra Red Spectroscopy (FTIR), Scanning Electron Microscope (SEM), Transmission Electron Microscope (TEM) and X-Ray Diffraction (XRD). Novelty of this present study is that the plant extract is very cost effective, eco-friendly; economic and effective alternative for the large scale synthesis of silver nanoparticles for antibacterial activity. The activity of the conjugates is still an open question and needs further study.

KEYWORDS: Green Synthesis, *Centella asiatica* L., Silver Nanoparticles (SNPs), Streptomycin (STP), Antibacterial Activity.

BIRENDRA KUMAR BINDHANI
School of Biotechnology, KIIT University, Bhubaneswar, Odisha, India

INTRODUCTION

In India, the use of different parts of several medicinal plants to cure specific ailments has been in vogue from ancient times [1]. India is rich in medicinal plant diversity. All known types of agro-climatic, ecologic and edaphic conditions are met within India. India is rich in all three levels of biodiversity, such as species diversity, genetic diversity and habitat diversity [2]. *Centella asiatica* L., a creeping plant in the family of Apiaceae, is found almost all over the world, including China, India and Thailand. This plant has been used in traditional folk healing for the ailments of a variety of conditions including headache, body ache, insanity, asthma, leprosy, eczemas, ulcers and wound healing [3, 4]. This plant also provides numerous beneficial effects for the nervous system such as anxiolytic [5] and anti-depression [6]. Recent studies both in animals and in human volunteers demonstrated that this medicinal plant could enhance cognitive function [7– 10], and is having antioxidant activity [11]. Nanoparticles are a particular group of materials with unique features and extensive applications in diverse fields [12]. Metal nanoparticle, such as silver has recognized significance in chemistry, physics and biology because of their unique optical, electrical, and photothermal properties [13]. The ease of synthesizing silver nanoparticle and its affinity for binding many biological molecules makes them attractive choice for study. Different physical and chemical methods have been reported over the last two decades for the synthesis of silver nanoparticle, of which chemical approaches, such as chemical reduction, electrochemical techniques, and photochemical reduction, are most broadly used. The green method of nanoparticle synthesis employing plant extracts is a easy and viable alternative to chemical procedures and physical methods [14]. Chemical and physical methods are harmful because the chemicals used are toxic, flammable, and are not disposed of simply in the environment [15]. In present years, biosynthesis of nanoparticles has received considerable attention due to the growing need to develop clean and nontoxic chemicals, environmentally friendly solvents, and renewable materials [16]. Utilization of biological systems such as plant extracts for the synthesis of nanoparticles has advantages over chemical and physical methods, because these systems are cost-effective, environment friendly, single-step in nature, and simply scaled up for large-scale synthesis [17].

Silver nanoparticles also reported to have anti-fungal [18], anti-inflammatory [19], anti-viral [20], anti-angiogenesis [21] and anti-platelet activity [22]. In recent times, the development of silver nanoparticles is expanding. Silver nanoparticles can be applied in coating for solar energy, bio-labelling, food packaging, antimicrobial agent and drug delivery [23, 24]. They are currently used as part of clothing, food containers, wound dressings, ointments, and implant coatings. Some silver nanoparticles applications have received consent from the US Food and Drug Administration [25]. Studies have revealed that the size, morphology, stability, and physicochemical properties of metal nanoparticles are powerfully influenced by the experimental conditions, [26-28] and play crucial roles in controlling the physical, chemical, optical, and electronic properties of these nanoscopic materials. This is mainly important for noble metal, such as silver, which has strong surface plasmon resonance oscillations [29]. The biological synthesis of silver nanoparticles is suitable and extracellular method which is environmentally safe. In the present study the silver nanoparticles were synthesized quickly by using the medicinal plants *Centella asiatica* L. against the cancer. Chavicol is present in *Centella asiatica* leaf. It is a phenolic compound and powerful reducing agent against metallic ion reduction [30]. At present, biosynthesis of SNPs were done using plant extracts of *Centella asiatica* L., although biosynthesis of silver nanoparticles by plants such as *Solanum xanthocarpum* L. *Berry* [31], *tea leaf* [32], *Callicarpa maingayi* stem bark [33] *Bauhinia variegate* [34], *Terminalia chebula* [35], *Trachyspermum ammi and Papaver somniferum* [36], *Hevea brasiliensis* [37], *Memecylon edule* [38], *Aloe vera* [39] have already been reported. However, the prospective of the plants as biological materials for the synthesis of nanoparticles is yet to be

fully explored. Though *Staphylococcus aureus* is responsible for many infections but it may also occur as a commensal. It can contaminate tissues when the skin or mucosal barriers have been breached. This can lead to many diverse types of infections including furuncles and carbuncles (a collection of furuncles). In infants, *Staphylococcus aureus* infection can cause a severe disease — staphylococca scalded skin syndrome (SSSS). *Staphylococcus aureus* infections can spread through contact with pus from an infected wound, skin-to-skin contact with an infected person by producing hyaluronidase that destroys tissues, and contact with objects such as towels, sheets, clothing, or athletic equipment used by an infected person. Deeply penetrating *Staphylococcus aureus* infections can be severe. Prosthetic joints can put a person at particular risk of septic arthritis, and staphylococcal endocarditis (infection of the heart valves) and pneumonia. *Staphylococcus aureus* can host phages, such as Panton-Valentine leukocidin, that increase its virulence [40, 41]. In the present research program green synthesis of silver nanoparticles were carried out using the leaf extract of *Centella asiatica* plant. Silver nanoparticles were produced through reduction of Ag containing salt namely $AgNO_3$ employing the natural precursor *Centella asiatica* as reductant. We have used *Centella asiatica* as reducing agent. Utilizing *Centella asiatica* is justified by its strong reducing capability. We describe and discuss the synthesis of Ag nanoparticles by employing the *Centella asiatica* leaf extract as reducing agent for $AgNO_3$. The reducing time with the *Centella asiatica* is small. A mechanism of reduction of $AgNO_3$ has been suggested based on detailed analysis of UV-Vis Spectrophotometer, XRD, FTIR, SEM, TEM and DLS. The antibacterial and antifungal activities of the nanoparticles have been investigated using a number of bacteria and fungus and the results seem to be very encouraging. It has been shown that the presence of OH- in *Chavicol* is able to release a proton and *Chavicol* itself changes into its anionic form. *Chavicol* acts as a very powerful reducing agent because of the inductive effect of two powerful electrons of the withdrawing methoxy and allyl group at ortho and para position of –OH group which enhances the proton releasing power of *Chavicol* (Figure-1).

Reduction of $AgNO_3$ by Centella asiatica L.

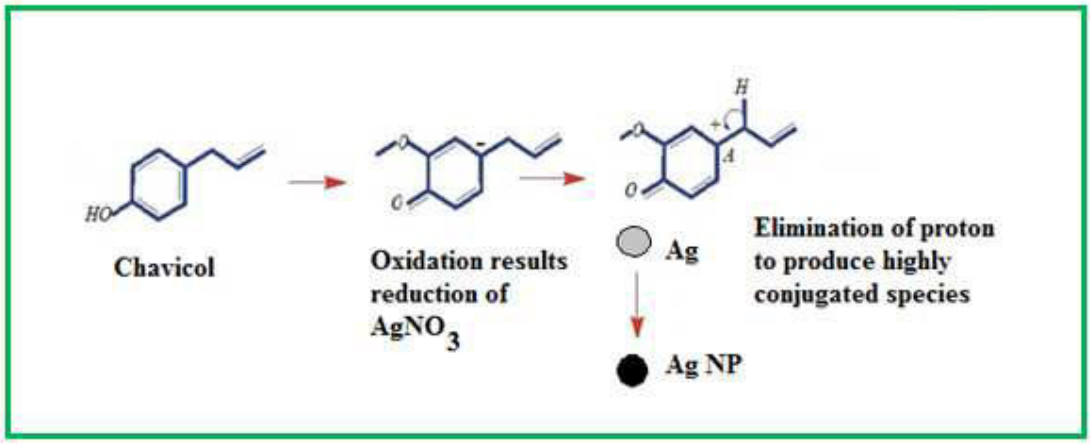

Figure 1
Schematic representation for the reduction of Ag ions

MATERIALS AND METHODS

Silver Nitrate ($AgNO_3$), Nutrient Agar was purchased from Sigma Aldrich. All reagents were commercial grade and were used without further purification. Water used in the experiment was ultrapure grade. *Centella asiatica* L. was collected from Regional Plant Research Centre (RPRC), Bhubaneswar,

Odisha, India.

Plant Material Collection

Centella asiatica L. leaves [Figure-2A] were collected from Regional Plant Research Centre (RPRC), Bhubaneswar, Odisha, India. The leaves were air dried for 10days, and then kept in the hot air oven at 60^{o}C for 24 to 48h. The leaves were ground to a fine powder.

Aqueous Extraction

Ten grams of air dried powder was placed in 100ml of organic solvent (90% methanol) in a conical flask, plugged with cotton and then kept on a rotary shaker at 180 to 200 rpm for 24hr. After 24hr., it was filtered through 4 layers of muslin cloth and centrifuged at 5000×g for 10 min. The supernatant was collected and the solvent was evaporated. The crude extract was diluted with 5% of DMSO (Dimethyl sulfoxide) to make the final volume one-tenth of the original volume and stored at 4^{0}C in air tight bottles for further studies [Figure-2C].

Synthesis of Silver Nanoparticles

Centella asiatica L. - Initiated and Stabilized Silver Nanoparticles at 40^{o}C (O-AgNo$_3^{-1}$)

1mM Silver nitrate [Figure-2B] was added to herb extract to make up a final solution of 200 ml and was centrifuged at 18000 rpm for 25min. The collected pellets were stored at 40^{o}C. A change in the colour of solution was observed during the heating process. Reduction of silver ion into silver particles during exposure to the plant extracts could be followed by colour change. Silver nanoparticle exhibited dark yellowish brown colour in aqueous solution due to the surface Plasmon resonance phenomenon [Figure-2D]. The silver nanoparticles thus formed were separated from residual and were characterized by UV-Vis absorption spectroscopy (O-AgNO$_3^{-1}$) [Figure-3].

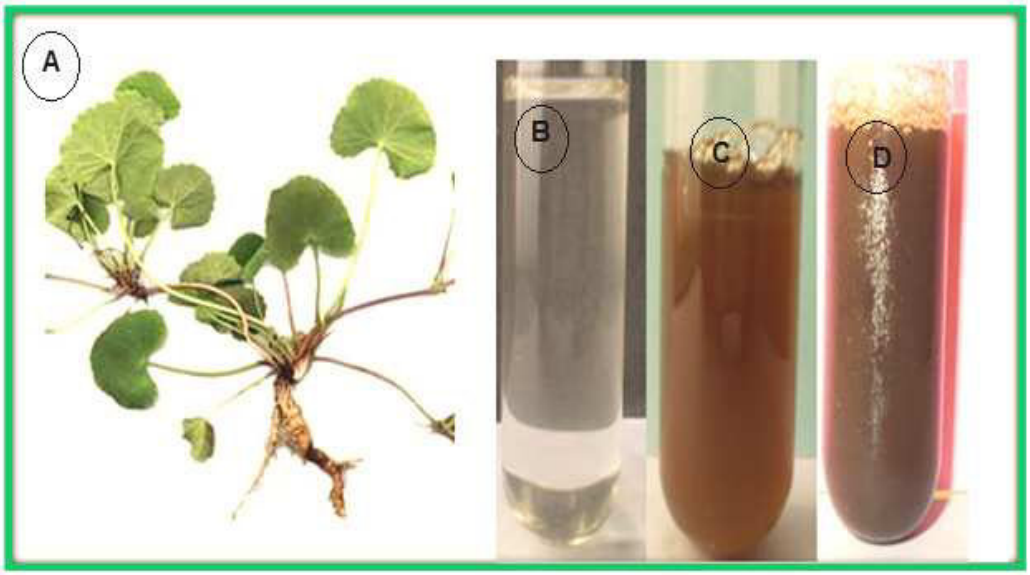

Figure 2

(A) Leaf of Centella asiatica L. (B) AgNO$_3$ Solution (C) Centella asiatica L. Leaf extracts. (D) Synthesis of Silver nanoparticles picture of aqueous solution of Centella asiatica leaf extracts.

Measurements

UV-Vis Spectroscopy

Ultraviolet-visible spectroscopy (UV-1601 pc shimadzu spectrophotometer) or ultraviolet-Visible spectrophotometer (UV-Vis) refers to absorption spectroscopy in the UV-Visible spectral region. This means it uses light in the visible and adjacent near-UV and near-infrared (NIR)) ranges. The absorption in the visible range directly affects the perceived colour of the chemicals involved. In this region of the electromagnetic spectrum, molecules undergo electronic transitions.

X-Ray Diffraction (XRD) Measurements

The phase formation of bio-reduced silver nanoparticles was studied with the help of XRD. The diffraction data of thoroughly dried thin films of nanoparticles on glass slides was recorded on D8 Advanced Brucker X-ray diffractometer with Cu K*α* (1.54 A^o) source.

Fourier Transmission Infra Red Spectroscopy (FTIR)

The FTIR spectrum of *Centella asiatica* L. extract, $AgNO_3$ nanoparticle and amine functionalized Ag nanoparticle were recorded by using BIORAD-FTS-7PC type FTIR spectrophotometer.

Scanning Electron Microscope (SEM) Analysis

Scanning Electron Microscope (SEM) analysis was done using Hitachi S - 4500 SEM machine. Thin films of the sample were prepared on a carbon coated copper grid by just dropping a very small amount of the sample on the grid, extra solution was removed using a blotting paper and then the film on the SEM grid were allowed to dry by putting it under a mercury lamp for 5 min.

Transmission Electron Microscope (TEM) Analysis

Transmission electron microscope (TEM) (Philips CM-10) is a microscopy technique whereby a beam of electrons is transmitted through an ultra-thin specimen, interacting with the specimen as it passes through. An image was formed from the interaction of the electrons transmitted through the specimen; the image was magnified and focused onto an imaging device.

Microbial Assay

Antibacterial activity was studied by the agar-well-diffusion method, wherein a bacterial suspension was added to sterile nutrient agar at 45^{o}C and the mixture was solidified on a Petri dish. A 20 ml volume of the medium was poured into a Petri dish (diameter, 90 mm) on a horizontally levelled surface. After the medium had solidified, 4-mm-diameter wells were made in the agars (at six wells per dish) that were equidistant from one another and from the dish edge. The wells received either 20 µL of the free antibiotic solution or 20 µL of the antibiotic–NP mixture. The Petri dishes were incubated at 37^{o}C for 24 h. After incubation, the diameter of the zone of bacterial-growth inhibition was measured with an accuracy of ± 0.1 mm. The mean inhibition-zone diameter and the maximal data scatter also were determined. All experiments were repeated thrice.

Bacterial Strain and Growth Conditions

Staphylococcus aureus (MTCC 9542) strain was maintained by School of Biotechnology, KIIT University, Bhubaneswar, Odisha, India. The strain was grown in Luria–Bertani (LB) broth medium at 37^{o}C. All inoculation experiments used an overnight accumulation culture grown to stationary phase in advance. The initial culture absorbance A600 was 0.04. Bacterial growth was assessed by using the time dependent absorbance curve. The cell concentration was estimated by the turbidity-spectra method.

CFU Enumeration

A bacterial suspension was mixed 1:1 with either a free Streptomycin (STP) solution or a Streptomycin (STP) – NP mixture and was incubated at 37^{o}C for 1 h. For each treatment, six 10-fold serial dilutions were made. A 200-µL volume of the resultant suspension was uniformly spreaded onto overnight dried solid LB medium with a sterile spatula. After cultivation at 37^{o}C for 24 h, all the colonies grown were enumerated, and the mean values and maximal scatter in CFUs were determined.

Table 1
Antibacterial action of Streptomycin (STP) and Streptomycin (STP) + NPs mixture on Staphylococcus aureus

Streptomycin (STP) concentration (mg mL^{-1})	Inhibition-zone diameter (mm)	
	Streptomycin (STP)	Streptomycin (STP) + NPs
0.563	9.8	9.9
1.13	11.5	11.8
2.25	12.14	12.11

RESULTS AND DISCUSSION

UV-Visible Absorption Spectra

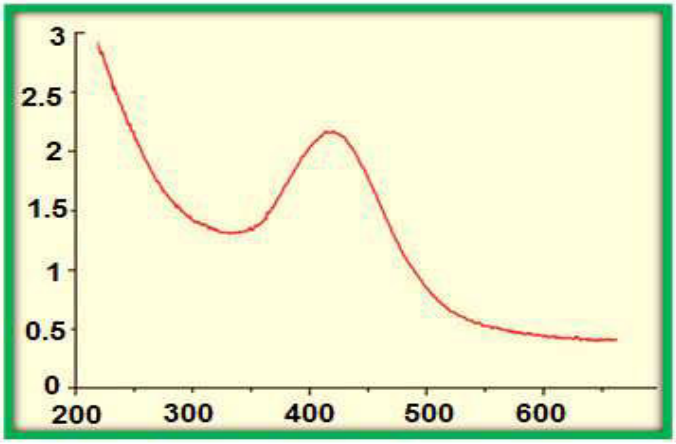

Figure 3
UV-Visible Absorption Spectra of O-AgNPs

The configuration of metal nanoparticles by reduction of the aqueous metal ions during exposure of *Centella asiatica* leaf extract was simply followed by UV–Vis spectroscopy (UV-1601 pc shimadzu spectrophotometer). UV-Vis absorption spectrum of silver nanoparticles in the presence of Ag/leaf extract is shown in figure 3. The Surface Plasmon band in the silver nanoparticles solution remains close to 430 nm throughout the reaction period, suggesting that the nanoparticles were dispersed in the aqueous solution with no evidence for aggregation in UV-Vis absorption spectrum.

X-Ray Diffraction (XRD) Measurement

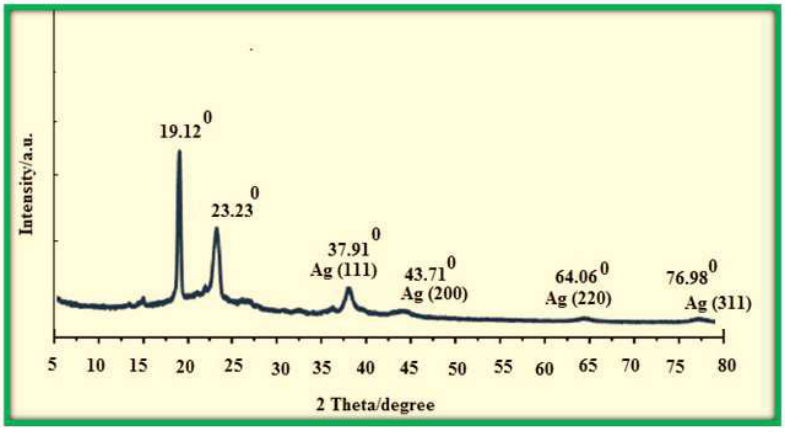

Figure 4
Representative XRD profile of Silver Nanoparticles

The formation of silver nanoparticles synthesized using leaf extract was further supported by X-ray diffraction (XRD) measurements (Figure - 4). It was observed that *Centella asiatica* leaf extract /Ag showed strong reflections at 2θ of 19.12° and 23.23°. For Ag/ leaf extract , the XRD peaks at 2θ of 37.91°, 43.71°, 64.06° and 76.98° were

characteristics to the (111), (200), (220), and (311) planes of the face-centered cubic (fcc) of Ag NPs, respectively. The peaks showed that the main composition of nanoparticles was silver and no obvious other peaks present as impurities were found in the XRD patterns. Therefore, this gives clear evidence for the presence of Ag NPs in the Ag/leaf extract. The (200), (220), (311) Bragg reflections are weak and considerably broadened relative to the intense (111) reflection. This interesting feature indicates that silver nano-crystals are in the film are predominantly (111)-oriented.

$$d = \frac{0.9\lambda}{\beta \cos \theta}.$$

Where 0.9 is the shape factor, generally taken for a cubic system, λ is the X-ray source wavelength, typically 1.54 Å, β is the full width at half the maximum intensity (FWHM) in radians, and θ is the Bragg angle. Using the above formula the crystallite size was calculated to be ~13 nm.

Fourier Transmission Infra Red Spectroscopy (FTIR)

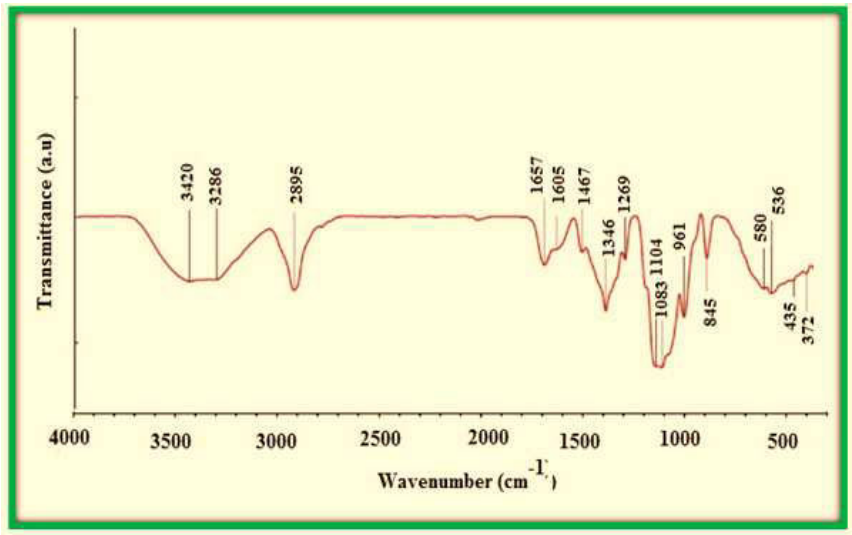

Figure 5
FTIR Spectrum of Ag Nanoparticles

FTIR measurements were carried out to recognize the possible biomolecules in the leaf extract responsible for the reduction of $AgNO_3^-$ ions (Figure - 5). The leaf of *Centella asiatica* contains 21% *Chavicol* (15) and the polyphenols and carboxylic compounds of *Centella asiatica* represents the FTIR spectrum of *Centella asiatica* leaf extract which shows prominent absorption bands at 1657 cm^{-1}, 1467 cm^{-1} and 3420 cm^{-1}. The shoulder at 1657 **c**m^{-1} is characteristic of carbonyl stretch vibrations from carboxylic acid and phenols, while the stretch at 1467 arises due to the C-O stretching and O-H deformation possibly from the acid groups present in the *Centella asiatica* leaf extract. The broad stretching at 3286 cm^{-1} arises due to the free O-H groups present in the phenols. Figure - 5, represents the FTIR spectrum of the *Centella asiatica* leaf extract reduced silver with the absorption bands at 1467 cm^{-1}, 1657 cm^{-1} and 3240 cm^{-1}. The shift in the carbonyl stretch frequency (1657 cm^{-1}) to

lower wavenumbers (1657 cm^{-1}) followed by the disappearance of the 1605 cm^{-1} resonance may be due to its binding with the silver nanoparticle surface. The shift in the C-O stretching and O-H deformation frequency (1467 cm^{-1}) to lower wave numbers (1467 cm^{-1}) followed by the disappearance of the 1467 cm^{-1} resonance indicate the facilitation of the binding of O-H group of phenols with the silver nanoparticle surface. In addition to above supportive evidence the 3286 cm^{-1} feature shifts to 2895 cm^{-1} due to the binding of the hydroxyl group with silver nanoparticle surface.

SEM (Scanning Electron Microscope)

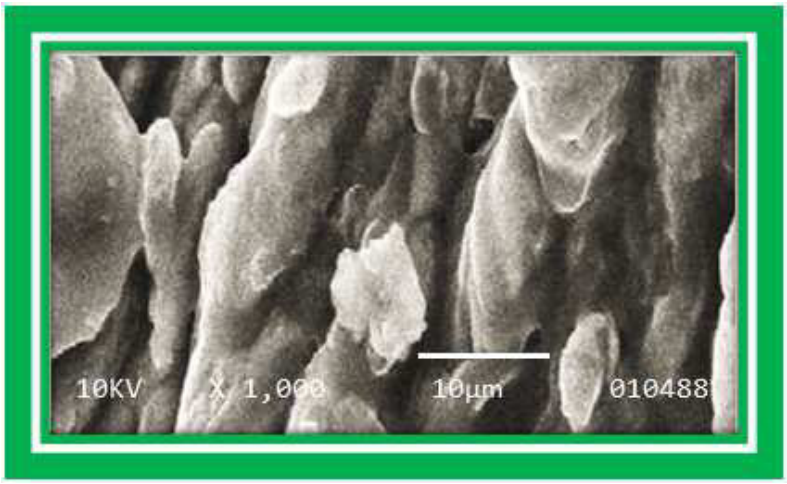

Figure 6
Micrograph of silver nanoparticles synthesised by the reaction of 1 mM silver nitrate with Centella asiatica L. leaf extract

Centella asiatica silver nanoparticles were subjected for the SEM analysis in which the SEM photos of silver nanoparticles and SEM photograph of *Centella asiatica* / silver nanoparticles clearly showed that in the room temperature synthesized samples (*Centella asiatica*), the size (diameter) of the nanoparticles lie between 30 - 50 nm. The average size of the nanoparticles is ~ 100 nm, and the shapes were spherical and cubic.

TEM

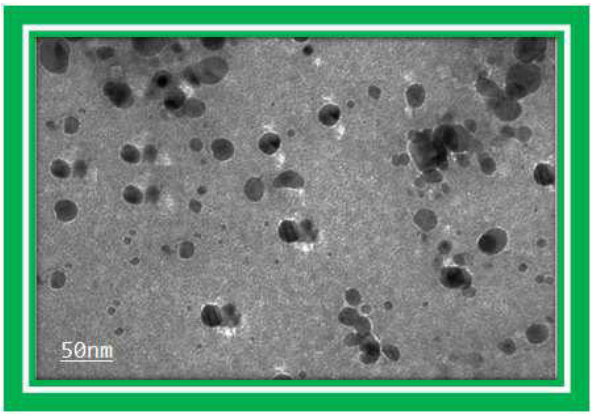

Figure 7
Silver nanoparticles synthesised by the reaction of 1 mM silver nitrate with Centella asiatica L. leaf extract

In this Figure – 7, showed the size of TEM image which gave a clear understanding of the morphology of functionalized AgNP synthesized using *Centella asiatica* L. leaves. The particles were almost spherical in shape having 30 - 50 nm sizes. The AgNP were spherical in shape, 15 - 45 nm range of in the size and found isolated in condition i.e., distributed uniformly. Absolute monodispersivity and couture the size could be achieved by making variations in the other factors like concentration of the salt solution, pH of the extract, and also changing the frequency for microwave irradiation during the conduction of the synthesis. The standard particles size measured from the TEM image which was in good agreement with the particle size calculated from XRD analysis.

Determination of the Minimum Inhibitory and Maximum Tolerant Concentrations

In experiments to determine the minimum inhibitory concentration (MIC) and the maximum tolerant concentration (MTC, equivalent to the ‘‘no observed effect concentration’’), culturing was done in micro-titration plate wells for 5 h. The initial culture absorbance A600 was 0.04. The MIC was taken to be the Streptomycin (STP) concentration at which the A600 of the bacterial suspension after incubation was almost the same as the initial A600, and the MTC was numerically equal to the Streptomycin (STP) concentration at which the parameters of culture growth were close to those for the control culture (without the antibiotic).

Effect of the NP Concentration

The absence of improvement of the antibacterial action of the antibiotic–NP conjugates may have been due to the low concentration of particles themselves. Therefore, we examined the effect of the silver NP concentration on the antibacterial action of the conjugates. For this purpose, antibiotic solutions having the same concentration were mixed with equal volumes of 0.1, 0.5, and 1.0 mM silver solutions in 2 mM K_2CO_3 before being added to the wells. Note that the silver concentration of as prepared 30-nm particles was about 0.3 mM. Accordingly, the mass/volume concentration is about 57 μg mL^{-1} or, equivalently, the particle-number concentration is about 1.4 X 10^{12} mL^{-1}. After the preparation of a concentrated stock solution, the above concentrations (0.1–1 mM) were obtained by corresponding dilutions. The results (Figure - 8) show that the antibacterial activity of the preparations decreased slightly with increasing particle concentration, but from a statistical analysis of the data, it follows that this effect is within the error and is not significant. Diffusion of free Streptomycin (STP) and its complexes with NPs into agar as said above, addition of the antibiotic to the NP sol led to aggregation, confirmed by changes in the colloid colour and extinction spectrum and also by direct TEM images. Consequently, the absence of enhancement of the antibacterial action of the conjugates and particles sediment from the antibiotic–NP mixtures could be explained by an inability of aggregated particles to penetrate into agar gel. To test this hypothesis, we poured 1.5% agar gel (in water) into 40-mm-diameter Petri dishes, made a well in the centre of each dish, and applied an NP solution and a Streptomycin (STP) –NP mixture to the wells. A day later, a red silver halo was clearly seen around the well in the case of the NP solution, whereas a brown precipitate at the well bottom in the case of the mixture (Figure - 9).

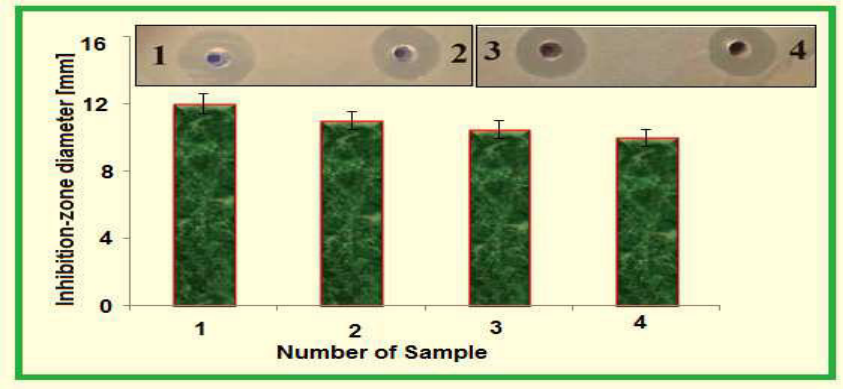

Figure 8

Zones of inhibition of the growth of Staphylococcus aureus upon application of Streptomycin (STP) (1) and Streptomycin (STP) –AgNP mixtures at particle concentrations of 0.1 (2), 0.5 (3), and 1.0 (4) mM and averaged inhibition-zone diameters for samples 1–4

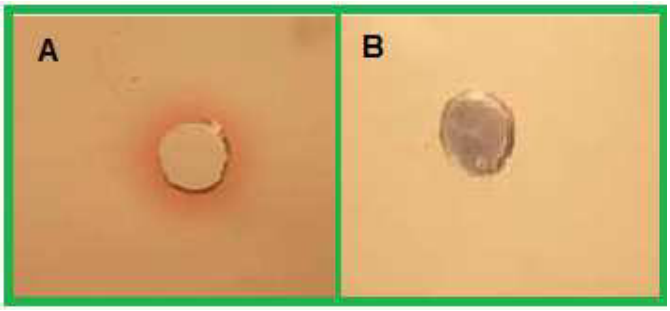

Figure 9

Petri dish with 1.5% agar gel at 24 h after application of an AgNP solution (A) and a Streptomycin (STP) –AgNP mixture (B).

In order to independently estimate the content of silver in the diffusion zones, we used AAS. Figure-9 showed that a spherical shaped portion of gel with an outer surface diameter of 15 mm and an inside diameter of 5 mm (the well diameter was 4 mm) was cut from the samples used for atomic absorption spectrometer (AAS) investigation of the silver contented in the gel. The same procedure was used for the gels which received the antibiotic– AgNP mixture and free AgNPs. Analysis showed that silver was totally absent in the agar gels around the mixture- containing wells but was present around the wells containing an AgNP solution (Table - 2).

Table 2

Analysis of silver content in the gel samples cut out around the wells at 24 h after the application of an AgNP solution and a Streptomycin (STP) – AgNP mixture.

Sample	Fraction of the total Ag mass in the sample (%)
Ag in 1.5% Agar Gel	9.3×10^{-4}
STP+ Ag in 1.5% agar gel	0
Ag in solid LB medium	3.3×10^{-4}
STP+ Ag in solid LB medium	0

Experiments with Bacterial Suspensions

Our study with bacteria grown on a solid nutrient medium has shown the absence of NPs in the inhibition zone. It follows that the question of enhancement of or decrease in the antibacterial activity of Streptomycin (STP) is meaningless in this context. Therefore, we decided to investigate the antibacterial activity

of an antibiotic–AgNP mixture in liquid culture, in which AgNPs or aggregates have a chance of coming in contact with bacterial cells because of Brownian motion. The antibacterial activity of the preparations was assessed by the MIC and MTC of Streptomycin (STP) and a Streptomycin (STP)–NP mixture for *Staphylococcus aureus*. From spectro-turbid-metric data, the initial cell density was 5 X 10^7 cells mL^{-1}. Figure 10, shows that the absorbance of the control culture in an AgNP-containing medium did not differ within the limits of error from that in an AgNP-free medium. The main result of this experiment is that curves 3 and 4 for bacterial cells grown with free Streptomycin (STP) and with a Streptomycin (STP) – NP mixture do not differ from each other. Consequently, the antibacterial activity of the Streptomycin (STP) – NP mixture does not exceed that of the native antibiotic not only on a solid nutrient medium, but also in a liquid medium. Quantitatively, this conclusion is shown in Table - 3, which gives data on the minimum inhibitory concentration (MIC) and maximum tolerant concentration (MTC) of the free antibiotic and its mixture with Ag NPs.

Table 3
The MICs and MTCs of Streptomycin (STP) and Streptomycin (STP) – NP mixture added to growing Staphylococcus aureus cells

Sample	MIC (lg mL^{-1})	MTC (lg mL^{-1})
STP	7.4	0.9
STP+ Ag	7.4	0.9

Comparison of the Bactericidal Effects of Streptomycin (STP) and Streptomycin (STP) – NP Mixture

In the final set of experiments, we compared the bacterial effects of the original antibiotic and a Streptomycin (STP) –NP mixture. For this purpose, the cells were placed on Streptomycin (STP) free solid LB medium from the 10^{-6} dilution of cultures incubated for 4 h with different preparations. For incubation, we used free Streptomycin (STP), a Streptomycin (STP) – AgNP mixture, and Ag NPs (control). The antibiotic concentrations were lowered by twofold dilutions from 240 to 3.7 μg mL^{-1}. The colony-forming units (CFU) data for the minimal and maximal values are given in Table 4. Table- 4, shows that Streptomycin (STP) at 240 μg mL^{-1} was bactericidal to 50 X 10^6 bacterial cells mL^{-1} both in a free state and in complex with AgNPs. The NPs decreased the CFU value, as compared with the control, but these differences were not significant. At a Streptomycin (STP) concentration of 3.7 μg mL^{-1}, the difference between the CFU values for free Streptomycin (STP) and for the mixture was almost twofold, with the addition of AgNPs decreasing, not increasing, the bactericidal action of the antibiotic. However, because the CFU method is usually in error by an order of magnitude, this difference between the CFU values for Streptomycin (STP) and for its mixture with NPs is not significant.

Table 4
The results of CFU counts after culturing on solid LB medium

Sample	CFU (cells mL^{-1})	
	240 μg of the antibiotic per ml	3.7 μg of the antibiotic per ml
Control	4.7 ± 0.4 X 10^9	4.5 ± 0.5 X 10^9
AgNPs	3.3 ± 0.8 X10^9	2.6 ± 0.3 X 10^9
STP	0	1.7 ± 0.3 X 10^9
STP+ NPs	0	0.9 ± 0.8 X 10^9

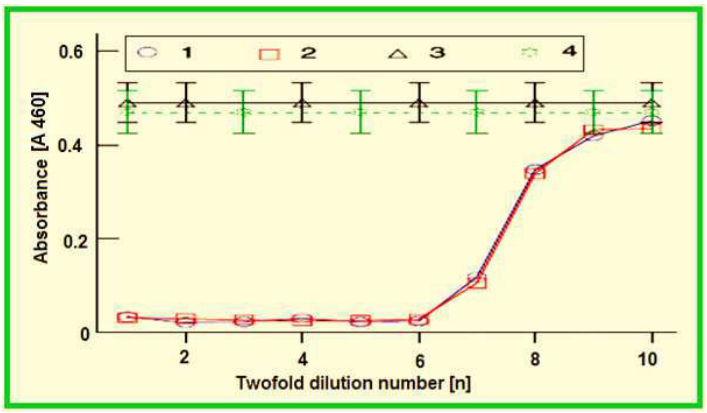

Figure 10

The absorbance (A460) of Staphylococcus aureus suspension after 4 h of incubation in LB nutrient medium versus the concentration of Streptomycin (STP) (1) and a Streptomycin (STP) – AgNP mixture (2). The x-axis shows two fold dilutions of the preparations. Lines 3 and 4 show the average absorbance level in the control medium (3) and in a Streptomycin (STP) free medium containing 0.1 mM NPs (4)

CONCLUSION

In this study, AgNPs were synthesized extra cellularly by *Centella asiatica* at room temperature. The AgNPs were quite stable without using any toxic chemicals as capping agents. The spherical AgNPs ranged in size from 30 - 50 nm, and showed promising broad-spectrum antimicrobial activity. The ability to synthesize AgNPs as potential anti-microbial agents using *Centella asiatica* is highly promising for the green, sustainable production of nano-metals, and this enhances its widespread application as an important strategy. Although Ag NPs themselves do not have any antimicrobial activity, they may act as drug carriers. In other words, because of the presence of Ag NPs, the surface area increases and hence it carries a lot of drug on its surface. Obviously, when the amount of drug in proximity of a bacterium is more, the antibacterial property may be enhanced. Applications of such nanoparticles in medical and other applications make this method potentially useful for the large-scale synthesis of other inorganic nano materials. In our opinion, the mechanism(s) of possible enhancement of the antibacterial activity of conjugates is still an open question and needs further study.

ACKNOWLEDGMENT

The authors are grateful to Department of Botany, Ravenshaw University, Cuttack, Odisha, India and School of Biotechnology, KIIT University, Bhubaneswar, Odisha, India for providing necessary laboratory facilities for this investigation. Authors also thank the CIPET, Bhubaneswar & Chennai for various analytical tests and encouragement.

REFERENCES

1. Bhattacharjee SK, Handbook of Medicinal Plants, Pointer Pub, Jaipur-03, India, pp. 1-6, (1998).
2. Zafar M, Iqbal A and Faiz M et al., Indian medicinal plants: a potential source for anticandidal drugs, J Ethnopharmacol, 37: 237-242, (1999).
3. T. K. Chatterjee, A. Chakraborty, M. Pathak, and G. C. Sengupta, “Effects of plant extract *Centella asiatica* (Linn.) on cold restraint stress ulcer in rats,” *Indian Journal of Experimental Biology*, 30 (10): 889–891, (1992).
4. L. Suguna, P. Sivakumar, and G. Chandrakasan, “Effects of *Centella asiatica* extract on dermal wound healing in rats,” *Indian Journal of Experimental Biology*, 34 (12): 1208–1211, (1996).

5. R. De Lucia, J. A. A. Sertie, E. A. Camargo, and S. Panizza, "Pharmacological and toxicological studies on *Centella asiatica* extract," *Fitoterapia*, 68 (5): 413–416, (1997).
6. Y. Chen, T. Han, L. Qin, Y. Rui, and H. Zheng, "Effect of total triterpenes from *Centella asiatica*on the depression behavior and concentration of amino acid in forced swimming mice," *Zhong Yao Cai*, 26 (12): 870–873, (2003).
7. M. H. Veerendra Kumar and Y. K. Gupta, "Effect of different extracts of *Centella asiatica* on cognition and markers of oxidative stress in rats," *Journal of Ethnopharmacology*, 79 (2): 253–260, (2002).
8. J. Wattanathorn, L. Mator, S. Muchimapura et al., "Positive modulation of cognition and mood in the healthy elderly volunteer following the administration of *Centella asiatica*," *Journal of Ethnopharmacology*, 116 (2): 325–332, (2008).
9. K. G. Mohandas Rao, S. Muddanna Rao, and S. Gurumadhva Rao, "*Centella asiatica* (L.) leaf extract treatment during the growth spurt period enhances hippocampal CA3 neuronal dendritic arborization in rats," *Evidence-Based Complementary and Alternative Medicine*, 3 (3): 349–357, (2006).
10. K. G. Mohandas Rao, S. Muddanna Rao, and S. Gurumadhva Rao, "Enhancement of amygdaloid neuronal dendritic arborization by fresh leaf juice of *Centella asiatica* (Linn) during growth spurt period in rats," *Evidence-Based Complementary and Alternative Medicine*, 6 (2): 203–210, (2009).
11. M. K. Zainol, A. Abd-Hamid, S. Yusof, and R. Muse, "Antioxidative activity and total phenolic compounds of leaf, root and petiole of four accessions of *Centella asiatica* (L.) urban," *Food Chemistry*, 81 (4): 575–581, (2003).
12. Matei A, Cernica I, Cadar O, Roman C, Schiopu V, Synthesis and characterization of ZnO-polymer nanocomposites, Int J Mater Form, 1:767–770, (2008).
13. Kemp MM, Kumar A, Mousa S, et al., Synthesis of gold and silver nanoparticles stabilized with glycosaminoglycans having distinctive biological activities. Biomacromolecules, 10:589–595, (2009).
14. Rivas L, Sanchez-Cortes S, Garcia-Ramos JV, Morcillo G., Growth of silver colloidal particles obtained by citrate reduction to increase the Raman enhancement factor. Langmuir, 17:574–577, (2001).
15. Zhang Z, Patel RC, Kothari R, Johnson CP, Friberg SE, Aikens PA., Stable silver clusters and nanoparticles prepared in polyacrylate and inverse micellar solutions, J PhysChem B., 104:1176–1182, (2000).
16. Chen W, Cai W, Zhang L, Wang G., Sonochemical processes and formation of gold nanoparticles within pores of mesoporous silica. J Colloid Interface Sci., 238:291–295, (2001).
17. Frattini A, Pellegri N, Nicastro D, de Sanctis O., Preparation of amine coated silver nanoparticles using triethylenetetramine, Mater Chem Phys., 94:148–152, (2005).
18. Kim K-J, Sung W, Suh B, et al., Antifungal activity and mode of action of silver nano-particles on *Candida albicans*, *Bio Metals*., 22(2), 235–242, (2009).
19. Nadworny P, Wang J, Tredget E, Burrell R., Anti-inflammatory activity of nanocrystalline silver-derived solutions in porcine contact dermatitis. *Journal of Inflammation*, 7(1), 13, (2010).
20. Lara H, Ayala-Nunez N, Ixtepan-Turrent L, Rodriguez-Padilla C., Mode of antiviral action of silver nanoparticles against HIV-1. *Journal of Nanobiotechnology*.; 8(1):1, (2010).
21. Kalishwaralal K, Banumathi E, Pandian SRK, *et al.,* Silver nanoparticles inhibits VEGF induced cell proliferation and migration in bovine retinal endothelial cells. *Colloids and Surfaces B: Biointerfaces*., 73(1): 51–57, (2009).
22. Shrivastava S, Bera T, Singh SK, Singh G, Ramachandrarao P, Dash D., Characterization of Antiplatelet Properties of Silver Nanoparticles, *ACS Nano*, 3(6): 1357–1364, (2009).
23. Philip D., *Mangifera indica* leaf-assisted biosynthesis of well-dispersed silver

nanoparticles, SpectrochimicaActa Part A: Molecular and Biomolecular Spectroscopy, 78(1): 327–331, (2011).
24. Kouvaris P, Delimitis A, Zaspalis V, Papadopoulos D, Tsipas SA, Michailidis N., Green synthesis and characterization of silver nanoparticles produced using Arbutus Unedo leaf extract, Materials Letters, 76(0): 18–20, (2012).
25. Atiyeh BS, Costagliola M, Hayek SN, Dibo SA., Effect of silver on burn wound infection control and healing: Review of the literature, *Burns*, 33(2): 139–148, (2007).
26. Knoll B, Keilmann F., Near-field probing of vibrational absorption for chemical microscopy, Nature, 399:134–137, (1999).
27. Sengupta S, Eavarone D, Capila I, Zhao GL, Watson N, Kiziltepe T., Temporal targeting of tumour cells and neovasculature with a nanoscale delivery system, Nature, 436:568–572, (2005).
28. Wiley BJ, Sun Y, Xia Y., Synthesis of silver nanostructures with controlled shapes and properties. Acc Chem Res., 40:1067–1076, (2007).
29. Kumar V, Yadav SK., Plant-mediated synthesis of silver and gold nanoparticles and their applications, J Chem Technol Biotechnol., 84:151–157, (2009).
30. Sutarjadi, H., Dymaik O, W., Santosa, M., Prayago, B., Studiawan, H., Sukardiman, H., Utilization of Ind one sian Traditional Plants for Pharmaceutical Purposes, Report of Research Project, Unpublished, (1994).
31. Amin M, Anwar F, Janjua MR, Iqbal MA, Rashid U., "Green Synthesis of SilverNanoparticles through Reduction with *Solanumxanthocarpum* L. Berry Extract", Characterization, Antimicrobial and Urease Inhibitory Activities against Helicobacter pylori, Int J MolSci, 13(8): 9923-41, (2012).
32. Loo YY, Chieng BW, Nishibuchi M, Radu S., "Synthesis of silver nanoparticles by using tea leaf extract from *Camellia Sinensis*", Int. J. Nanomedicine., 7: 4263 – 7, (2012).
33. Shameli K, Bin Ahmad M, Jaffar Al-Mulla EA, Ibrahim NA, Shabanzadeh P, Rustaiyan A, Abdollahi Y, Bagheri S, Abdolmohammadi S, Usman MS, Zidan M., "Green biosynthesis of silvernanoparticles using *Callicarpamaingayi* stem bark extraction", Molecules, 17(7): 8506-17, (2012).
34. Kumar V, Yadav SK., Synthesis of different-sized silvernanoparticles by simply varying reaction conditions with leaf extracts of *Bauhinia variegata* L., IET Nanobiotechnol, 6(1): 1-8, (2012).
35. Mohan Kumar K, Sinha M, Mandal BK, Ghosh AR, Siva Kumar K, Sreedhara Reddy P, Green synthesis of silver nanoparticles using *Terminalia chebula* extract at room temperature and their antimicrobial studies, Spectrochim Acta A Mol Biomol Spectrosc, 91: 228-33, (2012).
36. Vijayaraghavan K, Nalini SP, Prakash NU, Madhankumar D., "One step greensynthesis of silvernano/microparticles using extracts of *Trachyspermum ammi* and *Papaver somniferum*", Colloids Surf B Biointerfaces, 1 (94): 114-7, (2012).
37. Guidelli EJ, Ramos AP, Zaniquelli ME, Baffa O., Green synthesis of colloidal silver nanoparticles using natural rubber latex extracted from *Hevea brasiliensis*", Spectrochim Acta A Mol Biomol Spectrosc, 82(1): 140-5, (2011).
38. Elavazhagan T, Arunachalam KD. "*Memecylonedule* leaf extract mediated greensynthesis of silver and gold nanoparticles. "Int J Nanomedicine.; 6, 1265-78, (2011).
39. Panda S, Kar A., *Ocimum sanctum* leaf extract in the regulation of thyroid function in the male mouse, Pharmacol. Res, 38(2): 107-110, (1998).
40. Imolai N., "MRSA and the environment: implications for comprehensive control measures", *Eur. J. Clin. Microbiol. Infect. Dis.,* 27 (7): 481–93, (2008).
41. Curran JP, Al-Salihi FL., "Neonatal staphylococcal scalded skin syndrome: massive outbreak due to an unusual phage type", *Pediatrics,* 66 (2): 285–90, (1980).